International Journal of Engineering Research

Sirte University
Faculty of Engineering

Journal homepage: Scientific Journals (su.edu.ly)

Arc Vapor Deposition Coating of AlSi12 on Thin Austenitic Stainless Steel Wires: Parameter Optimization and Uniformity Study

Nasar A Ali[1], Alhammali A Younis[2]

Mechanical Engineering Department, Sirte University, Libya[1,2]

E-mail: N.A.ALI@su.edu.ly

ARTICLE INFOR

Article history:

Received 15 July 2026

Revised 02 August 2026

Accepted 15 August 2026

Available online

1 November 2026

ABSTRACT

This study investigates the deposition of AlSi12 coatings on thin stainless steel (1.4310) wires with a diameter of 0.2 mm using Arc Physical Vapor Deposition (Arc-PVD). The research was conducted in two stages: first, systematic optimization of deposition parameters on bulk stainless steel substrates, followed by coating application on thin wires using the optimized conditions. The coating parameters including bias voltage, arc current, argon pressure, and etching temperature were optimized through scratch adhesion testing to maximize coating-substrate adhesion. The optimal conditions were identified as a bias voltage of 30 V, arc current of 70 A, argon pressure of 0.06 Pa, and etching temperature of 450 °C, yielding critical loads of 10.8 N for duplex stainless steel (1.4410) and 9.7 N for austenitic stainless steel (1.4310). Subsequently, two thin wire coating configurations were evaluated: a dual cathode setup (cathodes positioned on the right and left sides) and a single cathode setup. Metallographic examination revealed that the dual-cathode configuration with sample rotation produced a uniform AlSi12 coating with an average thickness of 2.5 μm along the entire 30 cm wire length. In contrast, the single-cathode configuration resulted in non-uniform coverage, with coating observed only on the top and middle sections (1.5 μm average thickness) and virtually no deposition on the bottom section. These findings demonstrate that dual-cathode positioning is essential for achieving uniform coating distribution on thin wire substrates in Arc-PVD systems.

2026 Sirte University, All rights are reserved

Keywords: *Arc-PVD; AlSi12 coating; Thin wire; Coating uniformity; Adhesion test.*

1. Introduction

Lightweight composite materials are critical in modern manufacturing due to their unique combination of low density, high specific stiffness and strength, excellent corrosion resistance, and high thermal conductivity. The performance of these materials is fundamentally governed by the interfacial adhesion between the reinforcement and the matrix, as this interface serves as the primary load-transfer medium [1]. Surface coating of reinforcing wires has been widely adopted as an effective technique to improve wettability and promote chemical bonding or mechanical interlocking between stainless steel reinforcements and polymer matrices [2]. Stainless steel wires, despite their high strength and corrosion resistance, possess relatively smooth and chemically inert surfaces that restrict bonding to polymer matrices; surface coating has been widely adopted to modify surface roughness, chemical composition, and wettability, thereby enhancing interfacial adhesion and load transfer [3]. Among coating technologies, Arc Physical Vapor Deposition (Arc-PVD) has gained significant attention as a coating technique for composite reinforcement applications, combining high ionization rates and deposition rates with the ability to produce dense, adherent, and precisely controlled thin films exhibiting excellent coating-substrate adhesion [4]. These characteristics make Arc-PVD particularly suitable for coating applications requiring strong metallurgical bonding between the coating and substrate. However, the deposition of uniform coatings on geometrically complex or small-scale substrates, such as thin wires, presents substantial challenges due to the directional nature of vapor flux and the line-of-sight characteristics of the process [5]. In industrial-scale PVD operations, target positioning represents a major technical hurdle, as areas positioned at varying distances and angles from the evaporation source experience different flux densities, resulting in non-uniform coating thickness distribution. To address these challenges, PVD systems incorporate substrate rotation mechanisms and multi-source configurations to ensure uniform coating distribution across substrate surfaces [6].

Aluminum-silicon alloys, notably AlSi12, are widely employed as coating materials owing to their excellent corrosion resistance, low density, and good thermal properties [7]. Recent studies have demonstrated that Al-12Si coatings exhibit superior corrosion resistance compared to pure Al and lower-Si alloys, attributed to the dense network of eutectic silicon that obstructs corrosion from permeating through the aluminum matrix, while also providing the highest wear resistance under both uncorroded and corroded conditions. The corrosion resistance of Al-Si

alloys is influenced by the Si content, size, shape, and distribution, with higher Si content generally improving the barrier effect against corrosive media [8]. Although the deposition of AlSi12 coatings on stainless steel substrates has been extensively studied for bulk components, achieving uniform coating thickness on small scale cylindrical substrates such as thin wires remains challenging due to the directional nature of vapor flux and the resulting non-uniform flux distribution [9]. Stainless steel wires are extensively utilized in various engineering applications where both mechanical strength and corrosion resistance are required. The deposition of protective coatings on such wires can significantly expand their applicability in aggressive environments; however, achieving uniform coating thickness along the entire wire length necessitates careful optimization of both deposition parameters and system configuration [6, 10]. This study aims to optimize AlSi12 deposition parameters on stainless steel substrates and subsequently apply these conditions to coat thin austenitic stainless steel wires, focusing on the influence of cathode configuration (single versus dual cathodes) on coating uniformity along the wire length.

Deposition method

Arc Physical Vapor Deposition (Arc-PVD) was employed to deposit thin films onto stainless steel wires with a diameter of 0.2 mm. The deposition process was conducted using a 20 Interatom arc-PVD system (1987, USA), which consists of a water-cooled vacuum chamber, vacuum pumps capable of achieving a pressure of 1×10^{-3} mbar, arc evaporators (cathodes) with individual power supplies, DC and pulsed bias sources, a centrally mounted rotational drive (0–10.5 rpm) for the substrate holders, and an integrated process control system. The technical specifications of the system include a coating chamber volume of 130 dm^3 with a usable space of 190 mm in diameter and 410 mm in height, and is equipped with three evaporators at four installation sites operating at 27–40 V with an adjustable current of 35–100 A.

Substrate materials and their properties

Two types of stainless steel alloys were employed as substrate materials: duplex SS (1.4410), designated as "D", and austenitic chromium-nickel SS (1.4310), designated as "C", with their chemical composition, mechanical properties, and physical characteristics summarized in Tables 1 and 2, respectively.

Table 1: Chemical composition, mechanical and physical properties of SS 1.4310 [11].

Chemical Comp.		Mechanical Properties		Physical Properties	
Element	W%	Property	Value	Property	Value
C (max.)	0.15	•Tensile Strength (annealed)	516 [Mpa]	•Young's Modulus	192.9 [Gpa]
Mn (max.)	2				
Ni	6-8	•Yield Strength (annealed)	206 [Mpa]	•Density	7.9 [g/cm³]
P (max.)	0.045				
Cr	16-18	•Elongation in 2" %	40 [%]	•Specific Heat (0 - 100 °C)	500 [J/Kg°K]
Si (max.)	1				
S (max.)	0.03				

Table 2: Chemical composition, mechanical and physical properties of SS 1.4410 [12].

Chemical Comp.		Mechanical Properties		Physical Properties	
Element	W%	Property	Value	Property	Value
C	0.03	•Tensile Strength	795 [Mpa]	•Young's Modulus	200 [Gpa]
Mo	4				
Ni	7	•Yield Strength	550 [Mpa]	•Density	7.8 [g/cm³]
N	0.260				
Cr	25	•Elongation in 2" %	15 [%]	•Specific Heat	485 [J/Kg°K]

Samples preparation and coating

Substrate preparation and cleaning procedure

Prior to coating, small samples measuring 20 × 30 × 5 mm were sectioned using a hacksaw, ground and polished to achieve the required surface finish, and subsequently ultrasonically cleaned in an ethanol bath, as the surface morphology of the substrate significantly influences the properties of the deposited film, and this cleaning method offers several advantages including effective cleaning of difficult-to-access areas such as cavities and rough surfaces, environmental compatibility, and maintenance of the cleaning solution integrity.

Coating parameter optimization and adhesion testing

Following substrate preparation and surface cleaning, the coating process was conducted to establish optimal parameters for subsequent thin-wire coating. AlSi12 served as the coating material. The cathode was mounted at the top of the coating chamber, and Figure 1 illustrates the arrangement of the samples and cathode within the vacuum chamber during the optimization stage. Bias voltage, arc current, etching temperature, and chamber pressure were systematically varied to identify the optimal coating conditions.

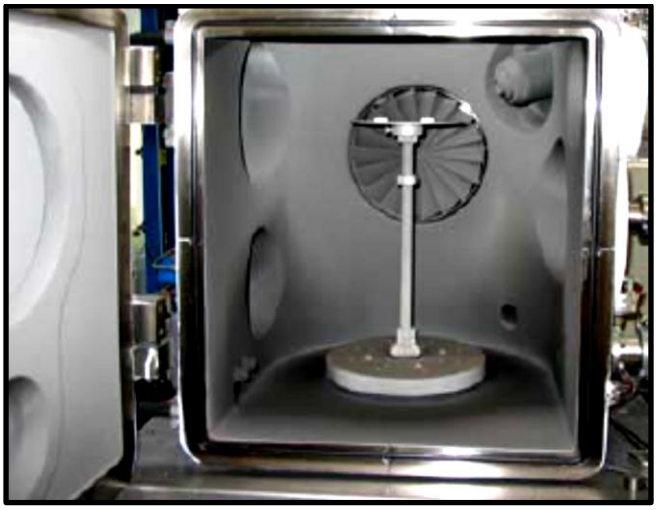


Fig. 1: Sample and cathode arrangement inside the arc-PVD coating chamber during parameter optimization.

AlSi12 cathode material

Table 3 presents the chemical composition of the AlSi12 alloy cathode (SINDLHAUSER MATERIALS, GmbH, Germany).

Table 3: Chemical composition of AlSi12[13].

Chemical composition	
Element	**W%**
Fe	0.01
Si	12
Cu	0.005
Pb	0.008
Zn	0.005
Ga	0.006
Au	0.002
Ti	0.003
Al	88

Coating parameter optimization

Table 4 presents the process parameters employed for AlSi12 coating optimization. The experimental design involved systematic variation of key parameters namely bias voltage, arc current, gas pressure, and etching temperature across four distinct optimization groups. At the conclusion of each coating group, scratch testing was performed to evaluate adhesion strength and thereby identify the optimal coating conditions.

Table 4: Process parameters for AlSi12 coating optimization.

1. Bias voltage optimization						
Samples No.	Bias voltage [V]	Current [A]	Etching temp. (°C)	Argon pressure [Pa]	Temperature [°C]	Coating time [Ah]
C4	30	55	450	0.5	<180	20
D4						
C5	40	55	450	0.5	<180	20
D5						
C6	50	55	450	0.5	<180	20
D6						
C13	60	55	450	0.5	<180	20
D13						
2. Current optimization						
Samples No.	Bias voltage [V]	Current [A]	Etching temp. (°C)	Argon pressure [Pa]	Temperature [°C]	Coating time [Ah]
C4	30	55	450	0.5	<180	20
D4						
C7	30	70	450	0.5	<180	20
D7						
C8	30	85	450	0.5	<180	20
D8						
C9	30	100	450	0.5	<180	20
D9						
3. Gas pressure optimization						
Samples No.	Bias voltage [V]	Current [A]	Etching temp. (°C)	Argon pressure [Pa]	Temperature [°C]	Coating time [Ah]
C10	30	70	450	0.06	<180	20
D10						
C11	30	70	450	0.1	<180	20
D11						
C7	30	70	450	0.5	<180	20
D7						
C12	30	70	450	1	<180	20
D12						
4. Etching Temperature optimization						
Samples No.	Bias voltage [V]	Current [A]	Etching temp. (°C)	Argon pressure [Pa]	Temperature [°C]	Coating time [Ah]
D2	30	70	350	0.06	<180	20
C2	30	70	400	0.06	<180	20
D14						
C1	30	70	450	0.06	<180	20
D15						
C3	30	70	500	0.06	<180	20
D3						

Wire coating procedure

SS 1.4310 thin wires with a diameter of 0.2 mm were coated using the previously optimized parameters. Achieving a uniform coating required careful consideration of the wire handling system, cathode configuration, and their positioning within the chamber. Initially, a thin steel sheet (1 cm in width) was employed as the handling system; however, to enhance coating uniformity, this mechanism was modified by replacing the sheet with hard wires (3 mm in diameter). Two cathodes were utilized for thin wire coating, positioned on the right, left, or front (door side) chamber walls. To further improve coating uniformity, the thin wire samples were rotated throughout the deposition process.

AlSi12 coating of thin wires

Using the optimal parameters determined previously, two thin wire samples were coated with an AlSi12 layer. The coating configurations for each sample were as follows:

- **Dual-cathode sample 1**: The sample was rotated during deposition, and two cathodes were employed, installed on the right and left sides of the coating chamber.
- **Single-cathode sample 2**: The sample was rotated during deposition, and a single cathode was employed, installed on the left side of the coating chamber.

Sample Characterization:

Adhesion Testing (Scratch Test)

The adhesion between the coating layer and the substrate was evaluated using the scratch test method. In this test, a spherical Rockwell-C diamond indenter is drawn across the coated sample surface under a continuously increasing normal load. As the load increases, the indenter produces progressive elastoplastic deformation in the film substrate system until damage occurs at the surface. The minimum load at which adhesion failure is first observed is defined as the critical load, which serves as a quantitative measure of the coating adhesion strength. Figure 2 illustrates the principle of the scratch test. Additionally, the morphology and thickness of the coating layer were examined through metallographic investigation using a light microscope.

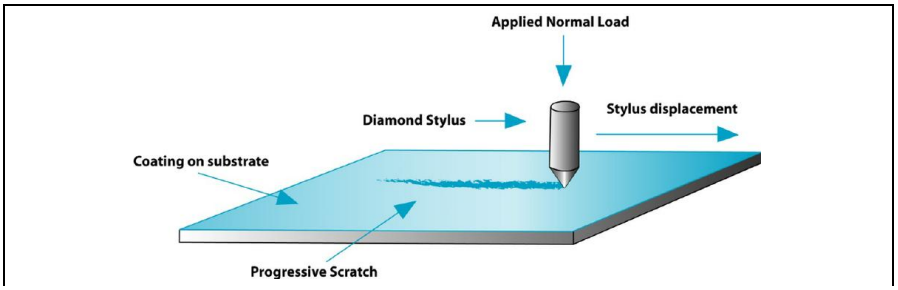


Fig. 2: Experimental setup for scratch adhesion testing[14] .

Sample Preparation

Accurate assessment of the coating microstructure required careful specimen preparation to avoid artifacts that could mask real material features. The workflow started with cold-mounting the cross-sectional specimen in epoxy resin. This step ensured mechanical stability and provided a flat reference surface for subsequent processing. The mounted specimens were then ground using silicon carbide (SiC) abrasive papers in descending order of coarseness: 320, 600, 1200, 2400, and 4000 grit. This multi-stage grinding sequence removed deformed layers from sectioning and produced a flat, uniform surface. Polishing was carried out in two stages. A rough-polishing phase used diamond suspensions (typically 3 µm and 1 µm) to remove residual grinding scratches. A fine polishing step followed, using sub-

micron alumina or colloidal silica to achieve a mirror like finish free of surface relief. After surface preparation was complete, optical microscopy was used for metallographic examination. This analysis revealed the coating layer's structural features, including its integrity, uniformity, and bonding with the substrate. Coating thickness was also measured precisely through calibrated image analysis.

Results and discussion

Coating Parameter Optimization

Scratch testing was performed on coated specimens to identify the optimal deposition parameters, with the parameter set yielding the highest adhesion (maximum critical load) designated as optimal. Two stainless steel substrates were employed: duplex SS (1.4410) and austenitic SS (1.4310). After samples were coated with the AlSi12 coating, Figure 3 illustrates the variation in critical load as a function of bias voltage during deposition.

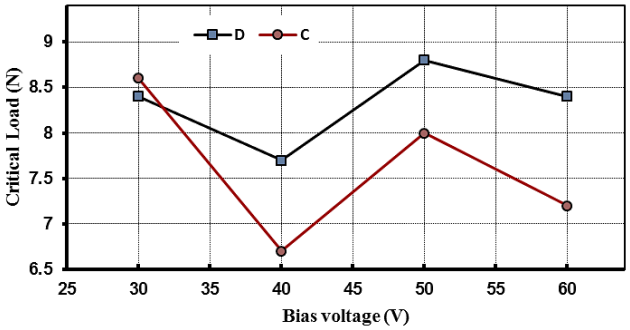


Fig. 3: Bias voltage vs. critical load for AlSi12-coated samples

Figure 3 shows that the highest critical load for both substrate types was achieved at the lowest bias voltage of 30 V, reaching 8.4 N for Sample D and 8.6 N for Sample C. The corresponding coating morphologies for these optimal conditions are presented in Figures 4 and 5, respectively.

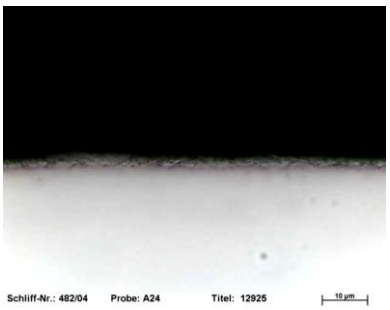


Fig. 4: Surface morphology of AlSi12 coating on Sample D deposited at the optimized bias voltage of 30 V, with an average thickness of 1.86 μm.

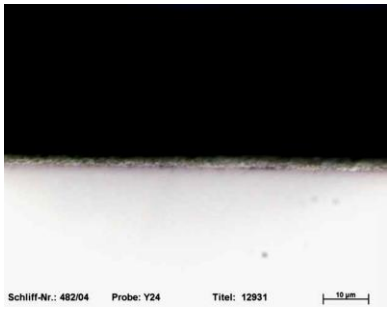


Fig. 5: Surface morphology of AlSi12 coating on Sample C deposited at the optimized bias voltage of 30 V, with an average thickness of 2.04 µm.

The current optimization was performed at the previously optimized bias voltage of 30 V. Figure 6 illustrates the variation of critical load with arc current for both substrate types.

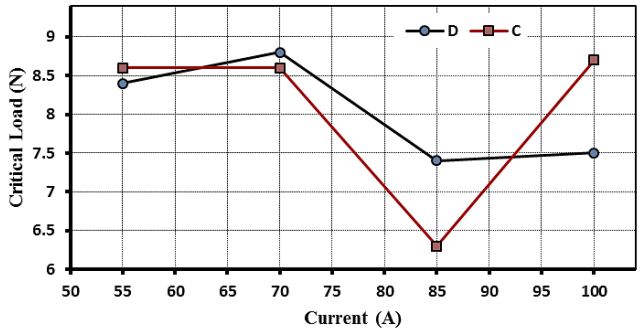


Fig. 6: Current vs. critical load for AlSi12-coated samples

Figure 6 illustrates the variation of critical load with arc current, where the highest critical load was obtained at the current value of 70 A (8.8 N for Sample D and 8.6 N for Sample C). Sample C exhibited a pronounced decline beyond this range, reaching a minimum of 6.3 N at 85 A, while Sample D remained relatively stable at higher currents. The corresponding coating morphologies are presented in Figures 7 and 8.

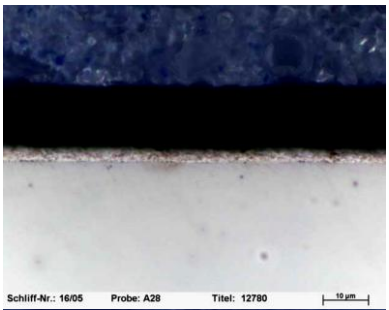


Fig. 7: Surface morphology of AlSi12 coating on Sample D deposited at the optimized current of 70 A, with an average thickness of 2.20 µm.

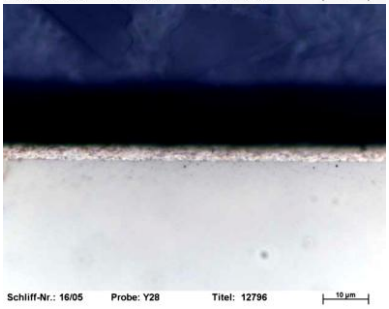


Fig. 8: Surface morphology of AlSi12 coating on Sample C deposited at the optimized current of 70 A, with an average thickness of 2.64 µm.

The argon pressure optimization was performed using the previously optimized current (70 A) and bias voltage (30 V) .Figure 9 presents the variation of critical load with argon pressure for both substrate types.

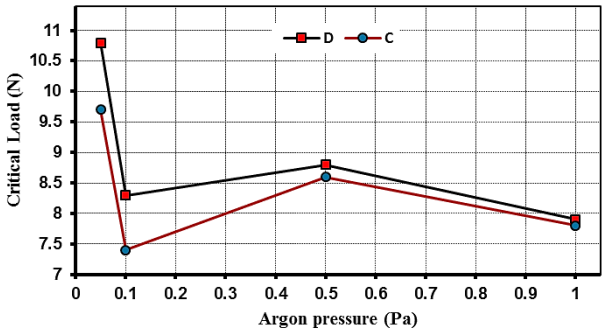


Fig. 9: Gas pressure vs. critical load for AlSi12-coated samples

Figure 9 shows that the highest critical load for both substrate types was achieved at the lowest argon pressure of 0.06 Pa, reaching 10.8 N for Sample D and 9.7 N for Sample C. Beyond this point, both samples experienced an initial sharp decline at 0.1 Pa, followed by partial recovery to comparable values of 8.6–8.8 N at 0.5 Pa, and a subsequent gradual decrease toward 1.0 Pa. The coating morphologies corresponding to these optimal argon pressure conditions are presented in Figures 10 and 11.

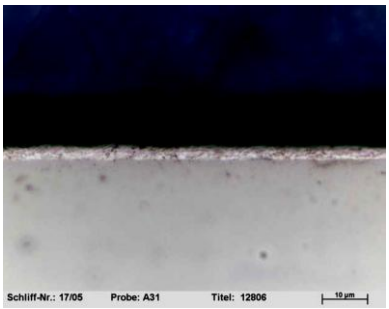


Fig. 10: Surface morphology of AlSi12 coating on Sample D deposited at the optimized argon pressure of 0.06 Pa, with an average thickness of 2.71 μm.

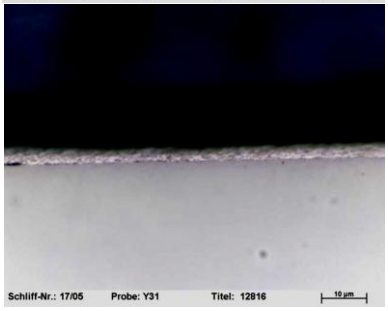


Fig. 11: Surface morphology of AlSi12 coating on Sample C deposited at the optimized argon pressure of 0.06 Pa, with an average thickness of 2.70 μm.

The etching temperature optimization was carried out using the previously established optimal values for current, bias voltage, and argon pressure. The relationship between critical load and etching temperature is shown in Figure 12.

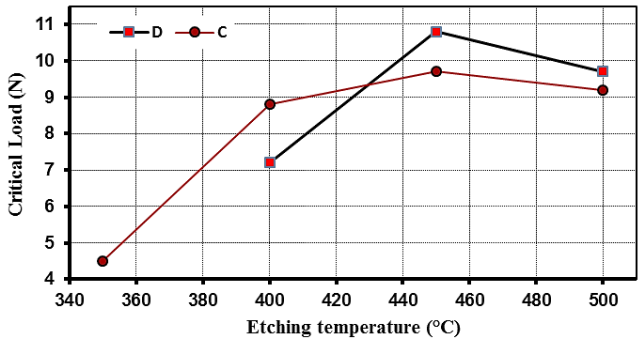


Fig. 12: Etching temperature vs. critical load for AlSi12-coated samples

Figure 12 shows that the critical load for both substrate types increases with etching temperature up to an optimal point. For Sample D, the critical load rose from 7.2 N at 400 °C to a peak of 10.8 N at 450 °C. Sample C exhibited a more pronounced improvement, increasing from 8.8 N at 400 °C, reaching 9.7 N at 450 °C, and maintaining a comparable value of 9.2 N at 500 °C. Thus, the highest critical load was obtained at the etching temperature of 450 °C for both samples, yielding 10.8 N for Sample D and 9.7 N for Sample C.

Based on the comprehensive optimization of AlSi12 coating parameters described above, the following optimal conditions were established:

Parameter	Value	Unit
Bias Voltage	30	V
Current	70	A
Argon pressure	0.06	Pa
Etching temp.	450	°C

These optimized parameters were subsequently employed to deposit AlSi12 coatings on thin steel wires.

Coating of Thin Wires with AlSi12

Thin stainless steel (1.4310) wires of 0.2 mm diameter were coated with AlSi12 using the optimal deposition parameters identified in this study. These parameters were kept constant during the process, while the position and number of cathodes were adjusted to achieve uniform coating. For this purpose, a 30 cm long wire sample was coated using two cathodes positioned on the right and left sides of the coating chamber, with the sample rotating around a fixed axis during deposition. To investigate coating uniformity, the sample was cut into three equal parts: bottom (PVD-S1), middle (PVD-S2), and top (PVD-S3). These segments were separately examined metallographically, and the results are shown in Figure 13 (a, b, and c).

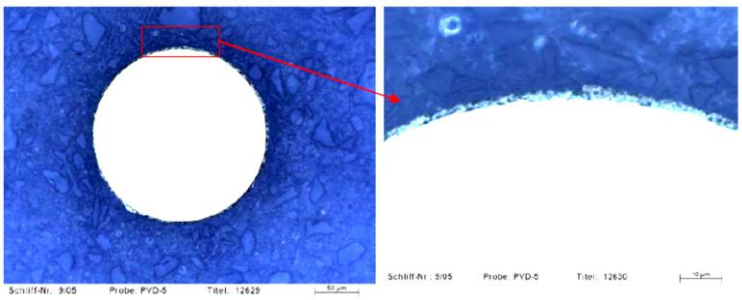


Fig. 13a: Optical micrograph of the bottom section (PVD-S1) of an AlSi12-coated thin steel wire.

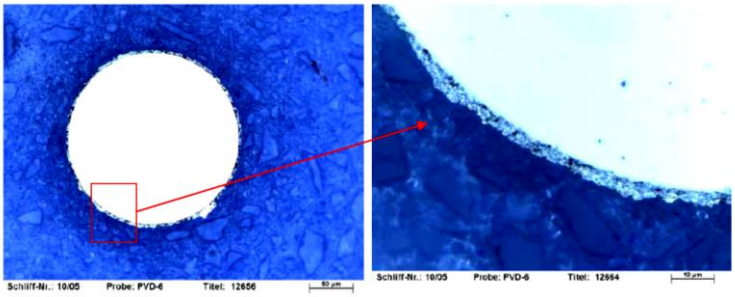


Fig. 13b: Optical micrograph of the middle section (PVD-S2) of an AlSi12-coated thin steel wire.

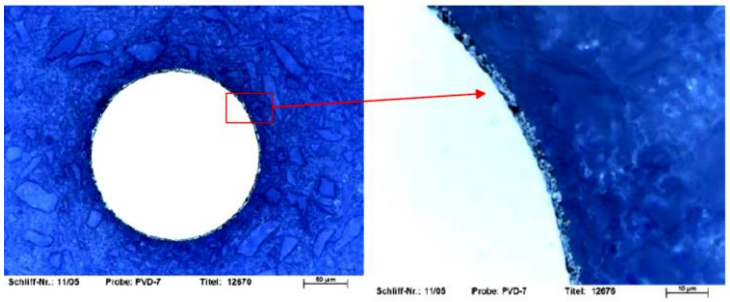


Fig. 13c: Optical micrograph of the top section (PVD-S3) of an AlSi12-coated thin steel wire.

In the first experiment, the coating was observed to be uniform, with an average thickness of 2.5 µm. No droplets were detected, which was attributed to the thin film nature of the coating. In the second experiment, a single cathode was employed and positioned on the left side of the coating chamber to evaluate the feasibility of achieving uniform coating with a single source. The sample was rotated around a fixed axis during deposition. For metallographic analysis, the coated wire was sectioned into three equal segments: bottom (PVD-S4), middle (PVD-S5), and top (PVD-S6). Each segment was examined separately, and the results are presented in Figure 14 (a, b, and c).

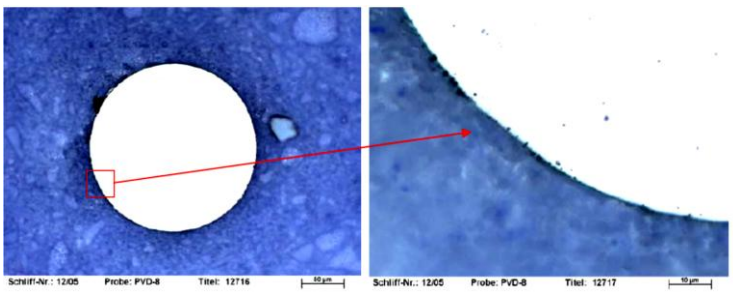


Fig. 14a: Optical micrograph of the bottom section (PVD-S4) of an AlSi12-coated thin steel wire.

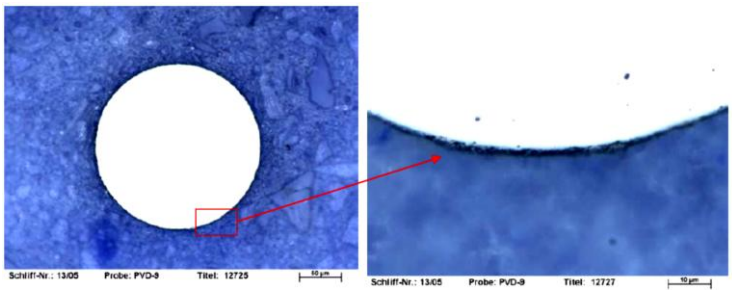


Fig. 14b: Optical micrograph of the middle section (PVD-S5) of an AlSi12-coated thin steel wire.

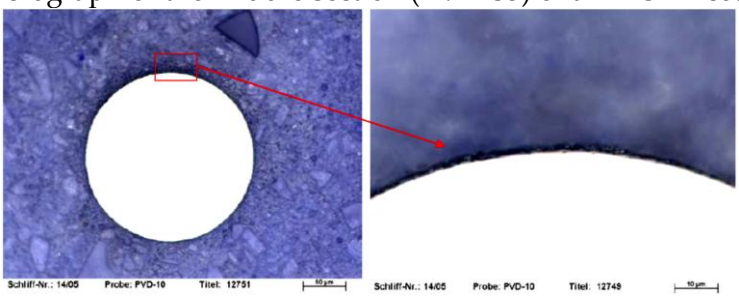


Fig. 14c: Optical micrograph of the top section (PVD-S6) of an AlSi12-coated thin steel wire.

The results presented in Figure 14 indicate that the coating was non-uniform along the length of the thin wire. Coating was observed on the top and middle sections with an average thickness of 1.5 µm, whereas the bottom section exhibited virtually no coating. This demonstrates that the use of a single cathode, even with sample rotation, is insufficient to achieve uniform coverage along the entire wire length, in contrast to the dual-cathode configuration employed in the first experiment.

Conclusions

1. Through systematic optimization using scratch adhesion testing, the optimal deposition conditions for AlSi12 coating were established as: arc current of 70 A, bias voltage of 30 V, argon pressure of 0.06 Pa, and etching temperature of 450 °C. These parameters yielded maximum critical loads of 10.8 N for duplex stainless steel (1.4410) and 9.7 N for austenitic stainless steel (1.4310), indicating good coating-substrate adhesion.

2. The application of optimized parameters to thin wire coating using a dual-cathode configuration (cathodes positioned on opposite sides of the coating chamber) with sample rotation resulted in a uniform AlSi12 coating along the entire 30 cm wire length. The coating exhibited an average thickness of 2.5 µm, and no droplets were observed, attributed to the thin film of the deposition.

3. The single-cathode configuration, despite sample rotation, failed to produce uniform coating along the wire length. Coating was present on the top and middle sections with an average thickness of 1.5 µm, while the bottom section showed

virtually no deposition. This non-uniformity is attributed to the directional vapor flux and the line of sight limitations inherent in the Arc-PVD process.

4. The results demonstrate that cathode configuration is a critical factor in achieving uniform coatings on thin wire substrates. The dual-cathode approach effectively overcomes the geometric constraints of wire coating by ensuring more comprehensive vapor flux coverage around the rotating substrate.

References

[1] W. D. Callister Jr and D. G. Rethwisch, Materials science and engineering: an introduction: John wiley & sons, 2020.

[2] Z. Li, H. Kong, M. Yu, S. Zhu, and M. Qin, "Coating strategy for surface modification of stainless steel wire to improve interfacial adhesion of medical interventional catheters," Polymers, vol. 12, p. 381, 2020.

[3] J. Sayyed, A. Ramprasad, and Y. Pai, "A review of fabrication techniques surface treatments and mechanical performance of stainless steel wire mesh reinforced polymer composites," Discover Materials, 2025.

[4] A. Voevodin and J. Zabinski, "Supertough wear-resistant coatings with 'chameleon'surface adaptation," Thin Solid Films, vol. 370, pp. 223-231, 2000.

[5] P. Zalm, J. Cuomo, S. Rossnagel, and H. Kaufman, "Handbook of ion beam processing technology," Noyes Publications, USA, 1989.

[6] Y. Wu, K. Liu, P. She, and J. Li, "Simulation and optimization of reactor airflow and magnetic field for enhanced thin film uniformity in physical vapor deposition," Microelectronic Engineering, vol. 296, p. 112294, 2025.

[7] J. R. Davis, Aluminum and aluminum alloys: ASM international, 1993.

[8] M. Kang, H. Kwon, E. Byon, and E. Lee, "Anti-corrosion and wear performance of Al-Si coating deposited by wire arc spray for marine applications," J. Adv. Mar. Eng. Technol, vol. 47, pp. 175-186, 2023.

[9] P. Eureka. (2023). Improving PVD Coating Uniformity Across Large Surfaces.

[10] M. Olsson and K. B. Surreddi, "Thin hard CVD and PVD coatings and their potential in steel wire drawing applications," in The 18th Nordic Symposium on Tribology-NORDTRIB 2018, Uppsala, 18-21 June 2018, 2018.

[11] B. EN, "10088–1. Stainless steels—part 1: list of stainless steels," British Standards Institution, 1995.

[12] O. E. ASTM, E. A. C. C. Ni, and M. SS, "Duplex Stainless Steel."

[13] https://www.fidat.it/en/aluminium-alloys/description-aluminum-alloys.html#AL-SI12-WR.

[14] https://www.researchgate.net/figure/Schematic-of-scratch-testing_fig1_276294463.